



HAL
open science

Localization, Morphologic Features, and Chemical Composition of Calciphylaxis-Related Skin Deposits in Patients With Calcific Uremic Arteriopathy

Hester Colboc, Philippe Moguelet, Dominique Bazin, Priscille Carvalho, Anne-Sophie Dillies, Guillaume Chaby, Hervé Maillard, Diane Kottler, Elisa Goujon, Christine Jurus, et al.

► To cite this version:

Hester Colboc, Philippe Moguelet, Dominique Bazin, Priscille Carvalho, Anne-Sophie Dillies, et al.. Localization, Morphologic Features, and Chemical Composition of Calciphylaxis-Related Skin Deposits in Patients With Calcific Uremic Arteriopathy. *JAMA Dermatology*, 2019, 155 (7), pp.789-796. 10.1001/jamadermatol.2019.0381 . hal-02291277

HAL Id: hal-02291277

<https://hal.sorbonne-universite.fr/hal-02291277>

Submitted on 18 Sep 2019

HAL is a multi-disciplinary open access archive for the deposit and dissemination of scientific research documents, whether they are published or not. The documents may come from teaching and research institutions in France or abroad, or from public or private research centers.

L'archive ouverte pluridisciplinaire **HAL**, est destinée au dépôt et à la diffusion de documents scientifiques de niveau recherche, publiés ou non, émanant des établissements d'enseignement et de recherche français ou étrangers, des laboratoires publics ou privés.

1 Original Investigation

2 **Localization, Morphology and Chemical Composition of Calciphylaxis-Related Skin**
3 **Deposits**

4 Running head: Characterization of calciphylaxis-related skin deposits

5 **Manuscript word count: 2902/3000; Table count: 1; Figure count: 4**

6 **Online supplement: eTable 1**

7

8 Hester Colboc, MD; Philippe Moguelet, MD;* Dominique Bazin, MD;* Priscille Carvalho,
9 MD; Anne-Sophie Dillies, MD; Guillaume Chaby, MD; Hervé Maillard, MD; Diane Kottler,
10 MD; Elisa Goujon, MD; Christine Jurus, MD; Marine Panaye, MD; Vincent Frochot, MD;
11 Emmanuel Letavernier, MD, PhD; Michel Daudon, MD; Ivan Lucas, MD; Raphaël Weil,
12 MD; Philippe Courville, MD; Jean-Benoit Monfort, MD; François Chasset, MD; Patricia
13 Senet, MD; on behalf of the Groupe Angio-Dermatologie of the French Society of
14 Dermatology

15

16 **Author Affiliations:** Sorbonne Université, Hôpital Rothschild, Service Plaies et Cicatrisation,
17 Paris (Colboc); Sorbonne Université, Hôpital Tenon, Anatomie et Cytologie Pathologiques,
18 Paris, (Moguelet); CNRS, Laboratoire de Chimie Physique, Ba340, Université Paris XI,
19 91405 Orsay (Bazin); Centre Hospitalier Universitaire de Rouen, Service de Dermatologie,
20 Rouen (Carvalho); Centre Hospitalier Universitaire d'Amiens, Service de Dermatologie,
21 Amiens (Dillies, Chaby); Centre Hospitalier du Mans, Service de Dermatologie, Le Mans
22 (Maillard); Hôpital Bichat, Service de Dermatologie, Paris (Kottler); Centre Hospitalier de
23 Chalon-sur-Saône, Service de Dermatologie, Chalon-sur-Saône (Goujon); Clinique du
24 Tonkin, Service de Médecine Vasculaire, Villeurbanne (Jurus, Panaye); Sorbonne Université,
25 Hôpital Tenon, Service des Explorations Fonctionnelles Multidisciplinaires, Paris (Frochot,

26 Letavernier, Daudon); Sorbonne Universités, UMR 8235, Paris (Lucas); CNRS, LPS, Ba510,
27 Université Paris XI, 91405 Orsay (Weil); Centre Hospitalier Universitaire de Rouen,
28 Anatomie et Cytologie Pathologiques, Rouen (Courville); Sorbonne Université, Hôpital
29 Tenon, Service de Dermatologie, Paris (Monfort, Chasset, Senet)—all in France.

30 *These authors contributed equally to this work.

31

32 **Corresponding Author:** Dr Hester Colboc, APHP, Service Plaies et Cicatrisation, Hôpital
33 Rothschild, 5, Rue Santerre, 75012 Paris, France. Phone: +33 (0)6 03 61 16 23;
34 (hester.colboc@aphp.fr)

35

36 **Funding sources:** None

37 **Conflicts of interest:** None declared

38 **Word count:** 2902/3000

39

40

41

42

43

44

45

46

47

48

49

50

51 **Key Points**

52 **Question** What are the precise localization, morphology and chemical composition of
53 calciphylaxis-related skin deposits?

54 **Findings** CUA calcifications are composed of pure calcium–phosphate apatite, always
55 located circumferentially, mostly in the intima of otherwise normal-looking vessels, and often
56 associated with interstitial deposits, unlike calcifications observed in cutaneous
57 arteriosclerotic vessels, which are associated with medial hypertrophy containing the
58 calcifications and no interstitial deposits.

59 **Meaning** The differences observed between CUA and cutaneous arteriosclerosis regarding
60 calcification location and vessel morphology suggest different pathogenetic mechanisms and
61 provide new insights into CUA pathogenesis that could explain the poor efficacy of
62 vasodilators and the therapeutic effect of calcium-solubilizing drugs.

63

64

65

66

67

68

69

70

71

72

73

74

75

76 **Abstract** 311/350

77 **IMPORTANCE** Calcific uremic arteriolopathy (CUA), a rare disease with calcium deposits
78 in skin, mostly affects dialyzed, end-stage renal disease patients. Chemical composition and
79 structure of CUA calcifications have been poorly described.

80 **OBJECTIVES** To describe the localization and morphology, determine the precise chemical
81 composition of CUA-related calcium deposits in skin, and identify any mortality-associated
82 factors.

83 **DESIGN** A retrospective, multicenter ~~case-control~~ study was conducted between January
84 2006 and January 2017.

85 **SETTING** Seven French hospitals participated in the study.

86 **PARTICIPANTS** This study included consecutive adults diagnosed with CUA, confirmed
87 according to Hayashi's clinical and histologic criteria. Patients with normal renal function
88 were excluded. For comparison, 5 skin samples from patients with arteriolosclerosis and 5
89 others from the negative margins of skin-carcinoma resections were also analyzed.

90 **MAIN OUTCOME(S) AND MEASURE(S)** Localization and morphology of the CUA-
91 related cutaneous calcium deposits were assessed with optical microscopy and field-
92 emission-scanning electron microscopy (FE-SEM), and the chemical compositions of those
93 deposits were evaluated with μ Fourier transform infra-red (FT-IR) spectroscopy, Raman
94 spectroscopy and energy dispersive X-ray (EDX).

95 **RESULTS** Thirty-six patients (median age: 64 years) were included, and 29 cutaneous
96 biopsies were analyzed. CUA and arteriolosclerosis skin calcifications were composed of pure
97 calcium-phosphate apatite. CUA vascular calcifications were always circumferential, found
98 in small-to-medium-sized vessels, with interstitial deposits in 76% of the samples. A
99 thrombosis, most often in noncalcified capillary lumens in the superficial dermis, was seen in
100 5 CUA patients' samples. Except for calcium deposits, CUA patients' vessel structure

101 appeared normal, unlike thickened arteriosclerotic vessel walls. Twelve (33%) patients died
102 of CUA.

103 **CONCLUSIONS AND RELEVANCE** CUA-related skin calcifications were exclusively
104 composed of pure calcium–phosphate apatite, localized circumferentially in small-to-
105 medium–sized vessels and often associated with interstitial deposits, suggesting its
106 pathogenesis differs from that of arteriosclerosis. Although the chemical compositions of
107 CUA and arteriosclerosis calcifications were similar, the vessels’ appearances and deposit
108 localizations differed, suggesting different pathogenetic mechanisms.

109

110

111

112

113

114

115

116

117

118

119

120

121

122

123 **Introduction**

124 Uremic calciphylaxis, also called calcific uremic arteriolopathy (CUA), is a rare and severely
125 morbid condition that predominantly affects dialyzed, end-stage renal disease (ESRD)
126 patients. Its frequency among ESRD patients reaches 4% and its incidence increases for those
127 on hemodialysis.¹ CUA's significant morbidity and mortality result from extensive skin
128 necrosis and septic complications, with the latter being the leading cause of death. For ESRD
129 patients, an increased risk of subsequent CUA development has been associated with female
130 sex, diabetes mellitus, higher body mass index, elevated serum calcium, phosphorus and
131 parathyroid hormone levels, nutritional status ~~in a cohort~~ or vitamin K-antagonist treatments.²

132 Although noninvasive imaging tools (eg, plain X-rays) have been reported to help
133 diagnose CUA,³ none of those tools have been systematically evaluated.⁴ Definitive CUA
134 diagnosis requires a skin biopsy. However, because biopsying the skin is associated with the
135 risk of new ulceration, bleeding and infection, actually obtaining one is ~~often discussed~~
136 sometimes debated.⁵ When obtained, deep cutaneous biopsies of CUA lesions show small-
137 sized calcifications, <500 μm , in hypodermal vessels and/or interstitial tissue, highly
138 suggestive of CUA with good specificity.⁶

139 Despite well-characterized clinical and histologic descriptions of CUA, its precise
140 pathogenetic mechanism remains unclear.⁷ Arteriolar calcification is probably the first event,
141 followed by thrombosis and skin ischemia. Chemical composition determination and
142 description of the skin calcifications through physicochemical techniques could contribute to
143 understanding CUA pathogenesis, leading to more appropriate and specific treatments.⁸
144 Indeed, nanotechnologies are receiving increased attention to improve understanding of the
145 effects of pathologic deposits on living tissues.^{9,10}

146 The aims of this study were to determine precisely the localization, morphology and
147 chemical composition of calcifications in the skin of CUA patients, and then examine whether

148 any association could be established between their microscopy findings and clinical
149 characteristics.

150

151 **Methods**

152 This study was conducted in compliance with Good Clinical Practices and the Declaration of
153 Helsinki, and in accordance with French law. Formal Ethics Committee approval of the study
154 protocol was obtained (no. EudraCT 2017-000906-39).

155

156 **Case Selection and Histopathologic Analyses**

157 This retrospective ~~case-control~~ study included consecutive adults diagnosed with CUA,
158 confirmed according to Hayashi's clinical and histologic criteria, and seen in 7 French
159 hospitals between January 2006 and January 2017.¹¹ Patients with normal renal function were
160 excluded. Patients' medical histories, treatments and laboratory findings were extracted from
161 their medical charts. They were classified into 2 clinical subgroups, distal or proximal CUA,
162 according to the skin-lesion localizations described by Brandenburg et al.¹²

163 Five skin samples from patients with arteriolosclerosis and 5 others from the negative
164 margins of skin carcinoma resections on the leg were included and served as controls. All 10
165 controls had normal renal function; only the 5 with arteriolosclerosis from among a cohort of
166 patients with necrotic angiodermatitis had leg-skin biopsies.

167 Skin-biopsy samples were sent to and centralized in Tenon Hospital, Department of
168 Pathology. For each subject, 1.5- μm -thick sections of paraffin-embedded skin biopsies were
169 deposited on glass slides, for hematoxylin-eosin-saffron (HES) and von Kossa staining, and
170 low-e microscope slides (MirrIR, Kevley Technologies, Tienta Sciences, Indianapolis, IN,
171 USA) for field-emission-scanning electron microscopy (FE-SEM), μ Fourier transform infra-
172 red (FT-IR) spectroscopy and Raman spectroscopy.¹³ Vascular and interstitial calcifications,

173 the calibers of calcified vessels and the topography of deposits in skin sections were analyzed
174 and compared between CUA patients and controls.

175

176 **FE-SEM**

177 FE-SEM (Zeiss SUPRA55-VP, Oberkochen, Germany) was used to describe the
178 ultrastructural characteristics of tissue sections. As previously described, high-resolution
179 images were obtained with in-lens and Everhart-Thornley secondary electron detectors.¹⁴
180 Measurements were taken at low voltage (1–2 kV), without the usual carbon-coating of the
181 sample surface. For some samples, energy-dispersive X-ray (EDX) was also used to identify
182 calcium in the abnormal deposits.

183

184 **FT-IR and Raman Spectroscopies**

185 Using the same sample as that for FE-SEM analyses, FT-IR and Raman spectroscopies
186 identified the chemical compositions of the CUA calcifications. All the FT-IR hyperspectral
187 images were recorded with a Spectrum Spotlight 400 FT-IR imaging system (Perkin–Elmer
188 Life Sciences, Courtaboeuf, France), with 6.25-mm spatial resolution and 8-cm⁻¹ spectral
189 resolution.¹⁶ Raman spectra were collected with a micro-Raman system (LabRam HR-800
190 Evolution, Horiba, Japan) using 785-nm laser excitation wavelength, 100× objective
191 (Olympus, numerical aperture 0.9) and 300 grooves per mm grating. Spectra were corrected at
192 baseline to suppress the strong luminescence background.¹⁵

193

194 **Statistical Analyses**

195 Data are expressed as median [range] or number (%). χ^2 or Fisher's exact tests were used to
196 compare qualitative variables; Wilcoxon or Mann–Whitney tests were used to compare paired
197 or nonpaired nonnormally distributed variables, respectively. Parameters with $P < .2$ in

198 univariate analysis were entered into a multivariate logistic-regression model, with *Y* as the
199 dependent variable.

200

201 **Results**

202 **Clinical and Histopathologic Findings**

203 Among the 36 CUA patients included, 29 skin biopsies could be analyzed by optical
204 microscopy, FE-SEM and spectroscopies. Clinical and histopathologic data are summarized
205 in Table 1.

206 Optical microscopy analysis of HES- and von Kossa-stained CUA biopsies always found
207 calcifications in small-and/or-medium-sized vessels (diameter: 10–300 μm), mostly in
208 hypodermal arterioles and capillaries (Figure 1). These deposits were massive, occupying in
209 the entire circumference of the vessel, and located in the intima and sometimes the media.
210 They could be associated with intimal fibrous or myxoid changes.

211 Those CUA vascular calcifications were associated with interstitial deposits, mainly
212 localized to the hypodermis, in 76% of the samples. Calcification size ranged from 1 to 500
213 μm , sometimes becoming confluent, with clusters reaching several millimeters in diameter.
214 They were either isolated small clusters between adipocytes (Figure 2A and B) or aligned in a
215 pearl collar along the cytoplasmic membranes of adipocytes (Figure 2D and E). Calcified
216 elastic fibers and/or collagen fibers were also seen in hypodermic septa or deep dermis.
217 Thromboses were seen in 5 samples, most often in noncalcified capillaries in the superficial
218 dermis.

219 The 5 arteriolosclerosis-control biopsies showed classical intimal fibrous endarteritis and
220 Monckeberg medial calcinosis associated with calcium deposits that were localized within the
221 media along the internal elastic lamina. Those calcifications were never circumferential and
222 no interstitial localization was observed. Negative margins of resected carcinomas contained

223 no vascular or interstitial calcium deposits.

224 Twelve (33%) patients died of CUA. Poorer CUA prognosis was only associated with
225 male sex or nodular lesions (eTable 1 in the supplement).

226

227 **FE-SEM and EDX Analyses**

228 Subcellular calcification localization and morphology were assessed with FE-SEM. CUA
229 vascular deposits were circumferential (Figures 1F and 2C); at least 1 thrombosis in 5/29
230 samples was located in the vessel lumen or intima, while the media usually appeared normal
231 with rare calcifications. Interstitial deposits surrounded adipocytes, along the cell membranes.
232 Morphologically, these calcifications appeared to be composed of aggregated micrometric
233 plates (Figure 2F).

234 FE-SEM analyses of control skin biopsies showing arteriosclerosis contained vascular
235 calcifications in the media (Figure 1C), associated with medial hypertrophy and intimal
236 fibrosis; no interstitial deposits were seen. FE-SEM analyses of negative resected carcinoma
237 margins confirmed the absence of vascular and interstitial deposits.

238 EDX analyses of CUA samples verified the calcium and phosphate composition of
239 vascular and interstitial deposits, with similar calcium/phosphate ratios in both sites. EDX
240 analyses showed the composition of vascular deposits in control arteriosclerosis biopsies to
241 be similar to that found in CUA.

242

243 **Spectroscopy Analyses**

244 FT-IR analyses of CUA and arteriosclerosis skin calcifications showed that all were
245 composed of calcium–phosphate apatite (Figure 3). Careful examination of 3 CUA samples
246 identified the presence of amorphous carbonated calcium–phosphate associated with calcium–
247 phosphate apatite that was not seen in any arteriosclerosis patients' samples.

248 Raman spectroscopy confirmed the similar calcium–phosphate-apatite compositions of
249 vascular and interstitial calcifications (Figure 4).¹⁶

250

251 **Discussion**

252 These FE-SEM, EDX and spectroscopy analyses were able to finally specify the localization
253 and the complete chemical composition of CUA patients' skin calcifications. Our
254 spectroscopic analyses demonstrated that those circumferential calcifications, located in the
255 intima and media of CUA patients' skin vessels, were composed exclusively of calcium–
256 phosphate apatite. In 76% of the CUA patients' samples, calcium–phosphate apatite was also
257 found in interstitial tissue of the deep dermis and hypodermis, along the cytoplasmic
258 membranes of adipocytes, and elastic and collagen fibers.

259 The chemical composition and localization of cutaneous CUA calcifications have been
260 investigated in only a few small series. Using EDX and FE-SEM, Kramann et al found
261 calcium/phosphate accumulations, with a molar ratio matching that of hydroxyapatite, in the
262 hypodermis of 7 CUA patients.¹⁷ Two other studies used mass spectrometry and Raman
263 spectroscopy to detect and characterize CUA skin calcifications. Using mass spectrometry,
264 Amuluru et al showed that tissue samples from 12 CUA patients had high iron and aluminum
265 contents, suggesting a role of metal deposition in CUA pathogenesis.¹⁸ Using
266 microcomputed-tomography and Raman spectroscopy, Lloyd et al confirmed the presence
267 carbonated apatite in debrided CUA tissues from 6 patients.¹⁹ However, those studies
268 included only small numbers of samples and performed only chemical analyses. To the best
269 of our knowledge, the precise localization and exact morphology of these abnormal deposits
270 have not yet been reported.

271 Patients with proximal lesions, high body mass index, ulcerated lesions and female were
272 reported to have poorer prognoses.²⁰ Our univariate and multivariate analyses did not identify

273 those factors as having a relationship with shorter survival, and retained only male sex and
274 nodular lesions as being significantly associated with mortality. However, the relatively small
275 number of patients included make those findings less relevant than risk factors identified in
276 larger studies.

277 Skin deposits in CUA and arteriosclerosis patients were always composed of calcium–
278 phosphate apatite, but their different localizations in the vessel walls could indicate different
279 pathogenetic mechanisms. Indeed, arteriosclerotic vessel walls are thickened, with media
280 hypertrophy, suggestive of slowly progressive thickening and degeneration of the arteriolar
281 wall with secondary calcium–phosphate apatite accumulation. Circumferential CUA vascular
282 deposits were located mostly in the intima of otherwise normal-looking vessels, suggesting a
283 faster and global process, with primary calcium deposition.

284 Ellis et al recently showed that pathognomonic cutaneous calcifications associated with
285 CUA could also occur in viable tissue from ESRD patients without CUA, ~~with ESRD~~
286 amputated because of peripheral arterial disease.^{21,22} However, Ellis et al did not consider that
287 some of their controls might have had undiagnosed acral calciphylaxis and undergone
288 amputations for distal ischemia. Those possibilities might explain some of their
289 histopathologic observations of calciphylaxis in their controls. ~~However,~~ Our histologic
290 findings (circumferential calcifications of small-to-medium-sized vessels often associated
291 with interstitial calcifications) and high-technology tools, such as FE-SEM, enabled us to
292 demonstrate several differences between the vascular calcifications seen in CUA and
293 arteriosclerosis, thereby confirming our previous results and those of Chen et al.^{6,23}

294 Patients with calciphylaxis probably develop skin calcifications subsequent to a
295 dysequilibrium between calcification promoters and inhibitors. Calcium-inhibitor deficiency,
296 like matrix Gla protein, impaired inhibition of calcium–phosphate precipitation, thereby
297 leading to skin calcifications.²⁰

298 Chronic inflammatory states, including ESRD, are associated with increased levels of
299 reactive oxygen species that impair endothelial function.²⁴ ESRD-related endothelial
300 dysfunction engenders vessel-wall abnormalities, including the presence of bone
301 morphogenetic protein in medial and intimal layers.²⁵ Such vascular protein modification,
302 associated with increased calcium × phosphate products, might explain the intimal and medial
303 calcifications observed in CUA.

304 Interstitial calcifications were also seen in 76% of CUA samples. Voluminous
305 calcifications of the subcutaneous tissue or dystrophic and metastatic calcinosis cutis are
306 known to occur in a variety of disorders, including dermatomyositis, lupus or trauma. The
307 ectopic calcified masses, composed of hydroxyapatite and amorphous calcium–phosphate
308 apatite, were disseminated throughout the dermis and hypodermis that appeared petrified,
309 involving interstitial tissue and vessels.²⁶ The pathophysiology is still unclear but it has been
310 hypothesized that hypodermal inflammation might release the phosphate bound to denatured
311 proteins and serve as a niche for ectopic calcifications.²⁶ However, despite clinical and
312 pathologic differences, the physiology of these calcifying disorders might be similar, and
313 calcium deposits obstructing some hypodermis vessels in CUA might lead to detrimental
314 adipocyte, collagen and elastic fiber alterations, and the release of the phosphate bound to
315 denatured proteins and ectopic interstitial calcifications. According to that hypothesis,
316 interstitial calcifications might be a secondary phenomenon, thereby explaining the inconstant
317 interstitial localization. The constant presence of vascular deposits could suggest a primary
318 vascular trigger of CUA.

319 Our finding that CUA vascular calcifications were always circumferential, suggests that
320 therapeutic strategies with vasodilators might be less relevant than those using calcium-
321 solubilizing drugs. Therefore, drugs directly impacting calcium–phosphate precipitation, like
322 sodium thiosulfate, bisphosphonates and vitamin K supplementation would seem to be more

323 appropriate and a rational approach for future therapeutic studies on CUA.^{27,28} Along the
324 same line, Dedinszki et al, who studied other calcifying disorders, including pseudoxanthoma
325 elasticum and generalized arterial calcifications of infancy, reported that oral pyrophosphate
326 inhibited tissue calcifications.²⁹

327 Because our study was retrospective, some information, including vital status was
328 missing for some patients. Our failure to identify factors associated with higher mortality in
329 larger studies might be explained by the relatively small size of our series. It is worth
330 highlighting that calcification morphology can be modified by the sectioning of paraffin-
331 embedded skin biopsies and that the appearance of these deposits may differ between glass
332 and low-e slides, making it more difficult to discern the relationship between optical
333 microscopy and electronic microscopy.

334

335 **Conclusions**

336 In conclusion, our histologic, FE-SEM, EDX and spectroscopy results provide a better
337 understanding of the morphologic, ultrastructural and chemical characteristics of CUA
338 patients' skin calcium-phosphate-apatite deposits. Those deposits appear to be initially
339 vascular and develop rapidly in normal vessel walls. Circumferential vascular and interstitial
340 deposits, albeit inconstant, were specific to CUA. Although the chemical compositions of the
341 calcifications were similar in CUA and arteriosclerosis, the vessels' appearances and
342 deposit localizations differed, suggesting different pathogenetic mechanisms.

343

344 **Acknowledgments**

345 Access to Data and Data Analysis

346 Hester Colboc had full access to all the data in the study and takes responsibility for the
347 integrity of the data and the accuracy of the data analysis.

348

349 The authors declared no conflicts of interest involving this work, no relevant financial
350 activities outside the submitted work (during the 3 years prior to submission) and no other
351 relationships or activities that readers could perceive to have influenced, or that give the
352 appearance of potentially influencing, what is written in the submitted work (based on all
353 relationships that were present during the 3 years prior to submission).

354

355 Funding/Support: no funding.

356

357 Role of Funder/Sponsor Statement

358 No funding organization or sponsor we involved in the design and conduct of the study;
359 collection, management, analysis, and interpretation of the data; preparation, review, or
360 approval of the manuscript; and decision to submit the manuscript for publication.

361

362 The authors thank LabEx MICHEM (ANR-11-IDEX-0004-02) for allowing us to use their
363 nano/micro-Raman facilities in UPMC. We thank Quentin Rezard from CNRS, LPC, Ba340,
364 Université Paris XI, and Chantal Jouanneau from INSERM, Hôpital Tenon, for their help and
365 support in this study

366

367

368 REFERENCES

- 369 1. Weenig RH, Sewell LD, Davis MD, McCarthy JT, Pittelkow MR. Calciphylaxis: natural
370 history, risk factor analysis, and outcome. *J Am Acad Dermatol*. 2007;56(4):569-579.
- 371 2. Nigwekar SU, Zhao S, Wenger J, et al. A nationally representative study of calcific
372 uremic arteriopathy risk factors. *J Am Soc Nephrol*. 2016;27(11):3421-3429.

- 373 3. Schmidt E, Murthy NS, Knudsen JM, et al. Net-like pattern of calcification on plain soft-
374 tissue radiographs in patients with calciphylaxis. *J Am Acad Dermatol*. 2012;67(6):1296-
375 1301.
- 376 4. Halasz CL, Munger DP, Frimmer H, Dicorato M, Wainwright S. Calciphylaxis:
377 comparison of radiologic imaging and histopathology. *J Am Acad Dermatol*.
378 2017;77(2):241-246.
- 379 5. Nigwekar SU, Kroshinsky D, Nazarian RM, et al. Calciphylaxis: risk factors, diagnosis,
380 and treatment. *Am J Kidney Dis*. 2015;66(1):133-146.
- 381 6. Cassius C, Moguelet P, Monfort JB, et al. Calciphylaxis in haemodialysed patients:
382 diagnostic value of calcifications in cutaneous biopsy. *Br J Dermatol*. 2018;178(1):292-
383 293.
- 384 7. Jean G, Terrat JC, Vanel T, et al. Calciphylaxis in dialysis patients: to recognize and treat
385 it as soon as possible. *Nephrol Ther*. 2010;6(6):499-504.
- 386 8. Bazin D, Daudon M, Combes C, Rey C. Characterization and some physicochemical
387 aspects of pathological microcalcifications. *Chem Rev*. 2012;112(10):5092-5120.
- 388 9. Colboc H, Moguelet P, Bazin D, et al. Physicochemical characterization of inorganic
389 deposits associated with granulomas in cutaneous sarcoidosis. *J Eur Acad Dermatol*
390 *Venereol*. 2019;33(1):198-203.
- 391 10. Bazin D, Daudon M. Pathological calcifications and selected examples at the medicine–
392 solid-state physics interface. *J Phys Appl Phys*. 2012;45(38):383001.
- 393 11. Hayashi M. Calciphylaxis: diagnosis and clinical features. *Clin Exp Nephrol*.
394 2013;17(4):498-503.
- 395 12. Brandenburg VM, Cozzolino M, Ketteler M. Calciphylaxis: a still unmet challenge. *J*
396 *Nephrol*. 2011;24(2):142-148.
- 397 13. Dessombz A, Bazin D, Dumas P, Sandt C, Sule-Suso J, Daudon M. Shedding light on the

- 398 chemical diversity of ectopic calcifications in kidney tissues: diagnostic and research
399 aspects. *PloS One*. 2011;6(11):e28007.
- 400 14. Brisset F. *Microscopie Électronique à Balayage et Microanalyses*. Paris, France: EDP
401 Sciences; 2012.
- 402 15. Carden A, Morris MD. Application of vibrational spectroscopy to the study of
403 mineralized tissues (review). *J Biomed Opt*. 2000;5(3):259-269.
- 404 16. Awonusi A, Morris MD, Tecklenburg MM. Carbonate assignment and calibration in the
405 Raman spectrum of apatite. *Calcif Tissue Int*. 2007;81(1):46-52.
- 406 17. Kramann R, Brandenburg VM, Schurgers LJ, et al. Novel insights into osteogenesis and
407 matrix remodelling associated with calcific uraemic arteriolopathy. *Nephrol Dial*
408 *Transplant*. 2013;28(4):856-868.
- 409 18. Amuluru L, High W, Hiatt KM, et al. Metal deposition in calcific uremic arteriolopathy.
410 *J Am Acad Dermatol*. 2009;61(1):73-79.
- 411 19. Lloyd WR, Agarwal S, Nigwekar SU, et al. Raman spectroscopy for label-free
412 identification of calciphylaxis. *J Biomed Opt*. 2015;20(8):80501.
- 413 20. Nigwekar SU, Thadhani R, Brandenburg VM. Calciphylaxis. *N Engl J Med*.
414 2018;378(18):1704-1714.
- 415 21. Ellis CL, O'Neill WC. Questionable specificity of histologic findings in calcific uremic
416 arteriolopathy. *Kidney Int*. 2018;94(2):390-395
- 417 22. Nigwekar SU, Nazarian RM. Cutaneous calcification in patients with kidney disease is
418 not always calciphylaxis. *Kidney Int*. 2018;94(2):244-246.
- 419 23. Chen TY, Lehman JS, Gibson LE, Lohse CM, El-Azhary RA. Histopathology of
420 calciphylaxis; cohort study with clinical correlations. *Am J Dermatopathol*.
421 2017;39(11):795-802.
- 422 24. Sowers KM, Hayden MR. Calcific uremic arteriolopathy: pathophysiology, reactive

- 423 oxygen species and therapeutic approaches. *Oxid Med Cell Longev*. 2010;3(2):109-121.
- 424 25. Nigwekar SU, Jiramongkolchai P, Wunderer F, et al. Increased bone morphogenetic
425 protein signaling in the cutaneous vasculature of patients with calciphylaxis. *Am J*
426 *Nephrol*. 2017;46(5):429-438.
- 427 26. Reiter N, El-Shabrawi L, Leinweber B, Berghold A, Aberer E. Calcinosis cutis: part I.
428 Diagnostic pathway. *J Am Acad Dermatol*. 2011;65(1):1–12.
- 429 27. Zitt E, König M, Vychytil A, et al. Use of sodium thiosulphate in a multi-interventional
430 setting for the treatment of calciphylaxis in dialysis patients. *Nephrol Dial Transplant*.
431 2013;28(5):1232-1240.
- 432 28. Nigwekar SU, Bloch DB, Nazarian RM, et al. Vitamin K-dependent carboxylation of
433 matrix Gla protein influences the risk of calciphylaxis. *J Am Soc Nephrol*.
434 2017;28(6):1717-1722.
- 435 29. Dedinszki D, Szeri F, Kozák E, et al. Oral administration of pyrophosphate inhibits
436 connective tissue calcification. *EMBO Mol Med*. 2017;9(11):1463-1470.

437

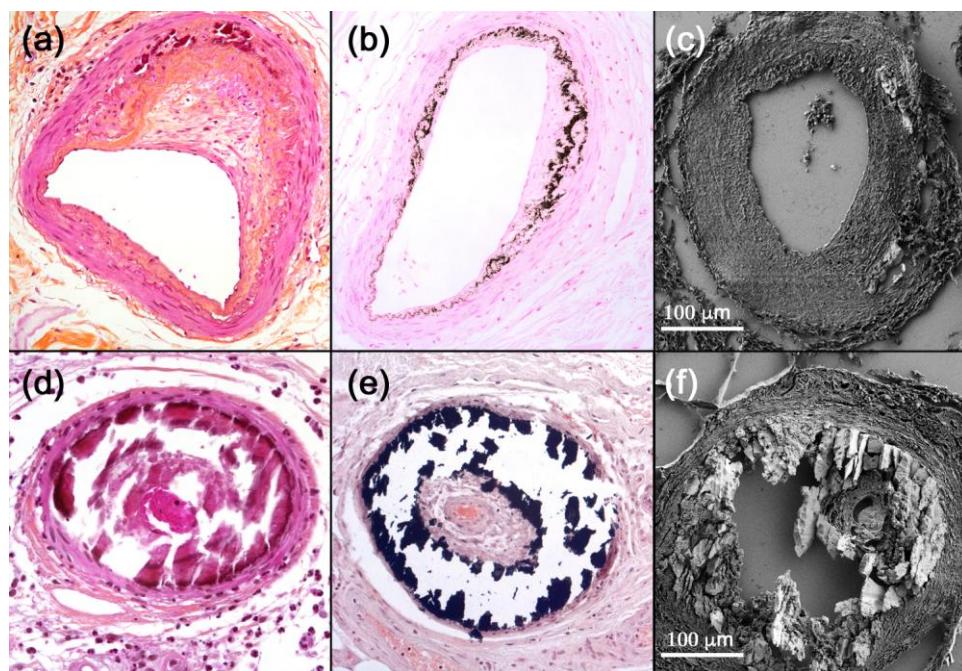
438

439

440 **Figure legends**

441 **Fig 1.** Skin biopsy sections. Arteriosclerosis with asymmetrical fibrous intimal thickening
442 (“fibrous endarteritis”) and Monckeberg medial calcinosis, ie, calcification of the internal
443 elastic lamina and media: A, hematoxylin–eosin–safron (HES)-stained (×400); B, von Kossa-
444 stained (×400); C, FE-SEM. Calcific uremic arteriolopathy (CUA) hypodermic arterioles with
445 voluminous and circumferential parietal calcium deposits: D, HES-stained (×400), E, von
446 Kossa-stained (×400); F, FE-SEM.

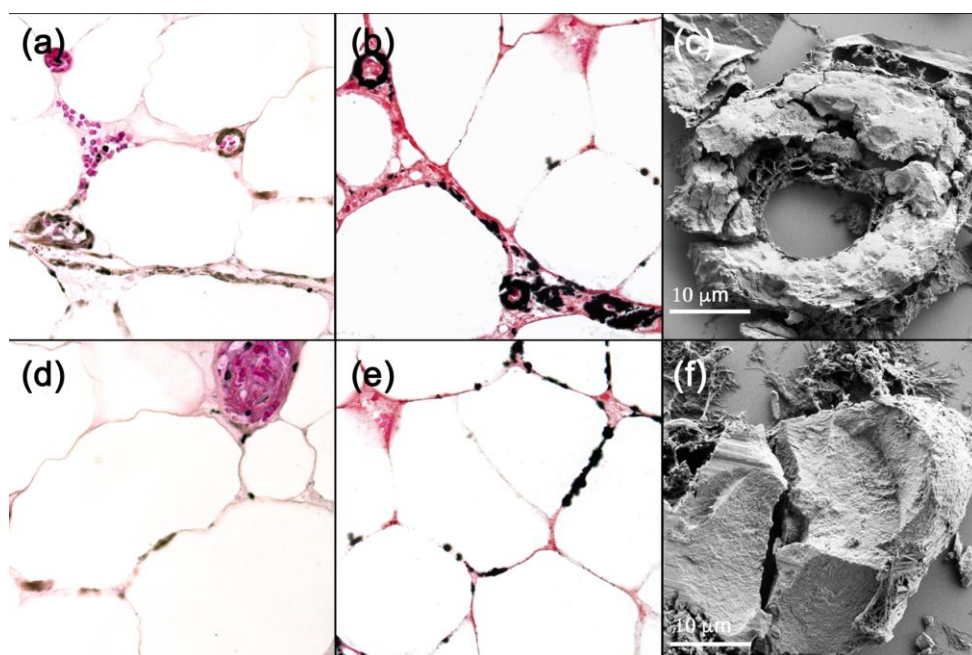
447



448

449

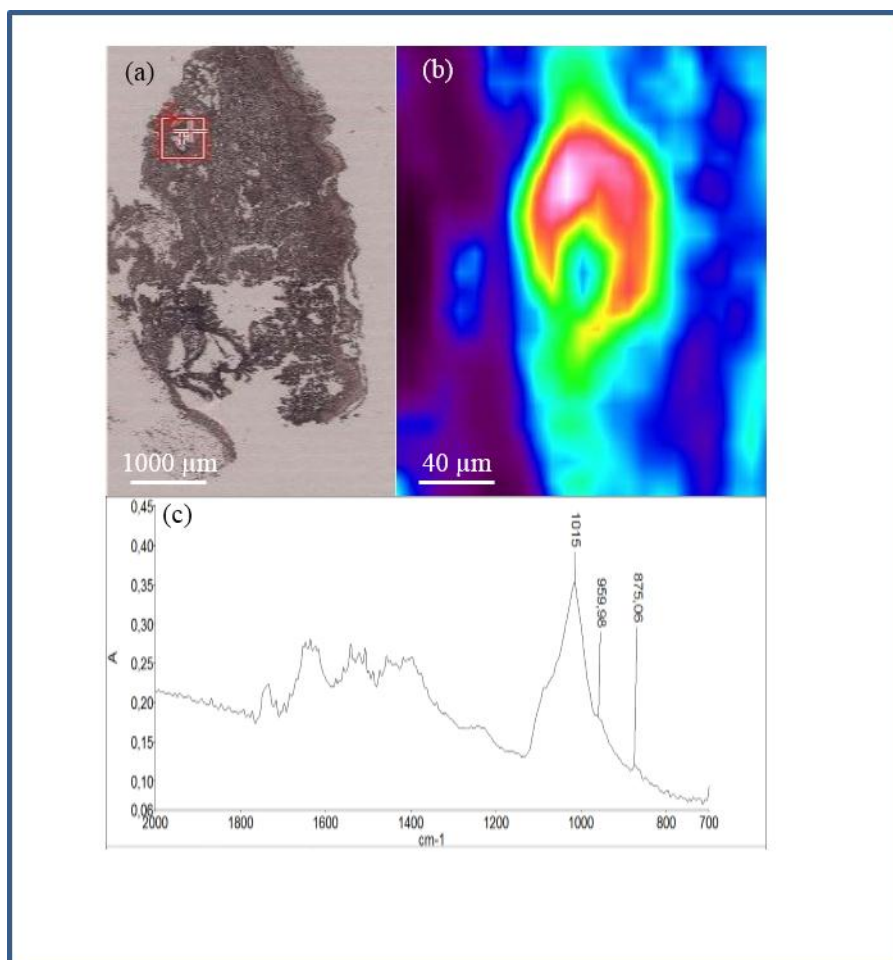
450 **Fig 2.** Skin biopsy sections. CUA hypodermic capillaries with voluminous and
 451 circumferential parietal calcium deposits: A, HES-stained ($\times 400$), B, von Kossa-stained
 452 ($\times 400$), C, FE-SEM. Interstitial CUA deposits, aligned along the cytoplasmic membranes of
 453 adipocytes: D, HES-stained ($\times 400$); E, von Kossa-stained ($\times 400$); F, FE-SEM.



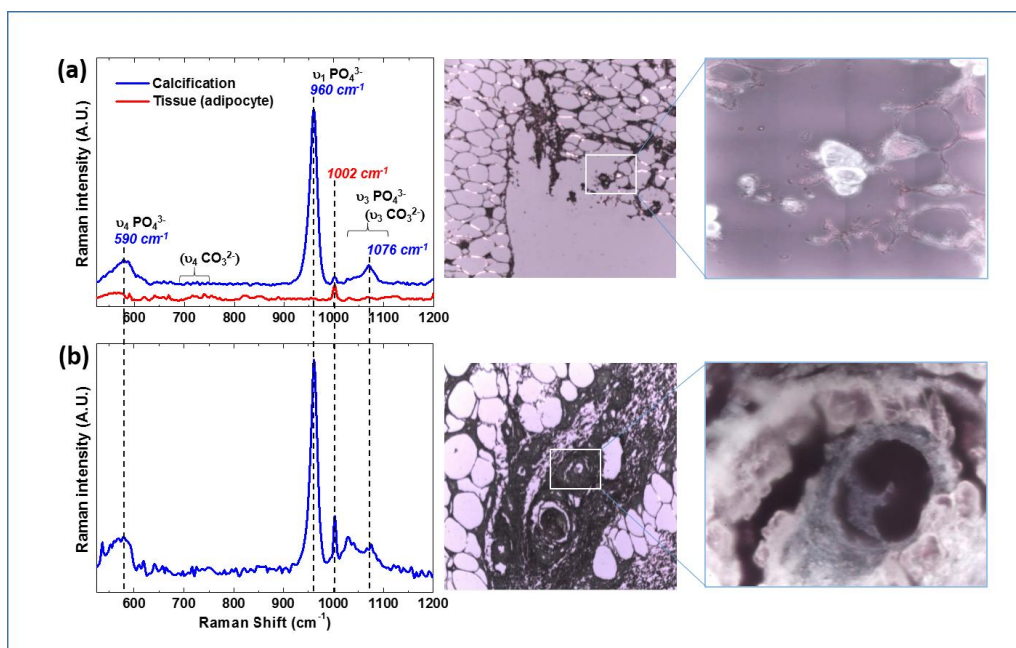
454

455

456 **Fig 3.** μ Fourier transform infra-red (FT-IR) spectroscopy of the interstitial CUA deposits: A,
 457 Skin biopsy of CUA; B, IR map of the red square area, showing an intense vascular deposit;
 458 C, IR spectrum of this vascular deposit: calcium–phosphate apatite spectrum with
 459 characteristic peaks (1015, 959 and 875 cm^{-1}) in a protein matrix (skin tissue). The same
 460 spectrum was obtained for CUA and arteriolosclerosis vascular calcifications.



461
 462 **Fig 4.** Micro-Raman signatures and optical micrographs (magnification 10 \times and 100 \times) of A,
 463 peri-adipocyte and B, vascular calcifications (excitation wavelength $\lambda_{\text{exc}} = 785 \text{ nm}$, objective
 464 100 \times , numerical aperture = 0.9). The Raman bands at 960, 1076 and 590 cm^{-1} correspond,
 465 respectively, to the ν_1 , ν_3 and ν_4 phosphate vibrations of apatite. The low-intensity ν_4
 466 carbonate vibrations around 680–715 cm^{-1} , expected for carbapatite, are not observed. The
 467 strong fluorescence background has been corrected on the presented spectra.



468

469

470 **Table 1** Baseline clinical, biologic and histologic characteristics of the 36 CUA patients

Characteristic	Value
Demographic	
Female/male ratio	2.6
Age at diagnosis, years	64 [33–89]
Comorbidity	
Dialysis	30 (83%)
Dialysis-to-CUA interval (months)	24 [1–156]
Diabetes	23 (64%)
Hypertension	33 (92%)
Body mass index >30 kg/m ²	14 (39%)
Vitamin K antagonists	16 (44%)
Clinical	
Proximal CUA	10 (28%)

Necrosis	26 (72%)
Ulceration	24 (67%)
Livedo reticularis	18 (50%)
Indurated plaques	15 (42%)
Nodular lesions	9 (25%)
Biologic	
Serum calcium, mmol/L	2.26 [1.89–2.84]
Serum phosphate, mmol/L	1.57 [0.93–3.68]
Calcium × phosphate product >4.5 mmol ² /L ²	12 (33%)
Serum parathormone >90 ng/L	24 (67%)
Serum albumin (median), g/L	28 [18–37]
Cutaneous histology	29
Vascular calcifications	29 (100%)
Interstitial calcifications	22 (76%)
Thrombosis	5 (14%)

471 Values are expressed as *n* (%) or median [range], unless stated otherwise. CUA, calcific

472 uremic arteriopathy

473

474

475

476

477

478

479

480

481

482

483

484

485

486

487

488

